Some Measurements on Dynamic Stall

A. G. Parker* and J. Bicknell†
Texas A&M University, College Station, Texas

Details of a flow oscillation device and of force and moment measurements on a 2 ft chord two-dimensional NACA 0012-64 airfoil in the oscillating flow and oscillated in pitch in a steady flow through stall are presented. Results indicate that both methods give essentially the same description of the dynamic stall process. It is apparent from peaks in the pressure distributions and in the pitching moment traces that more than one vortex is shed from the leading edge during the stall process. This, coupled with the very rapid changes that occur during stall, requires very close scrutiny of force and moment data that has not been recorded continuously. Understanding of dynamic stall overshoot will not be complete until detailed measurements are obtained in the region of the laminar separation bubble near the nose.

Nomenclature

c = chord (ft)
C_M = pitching moment coefficient
C_N = normal force coefficient
C_p = pressure coefficient
C_T = thrust coefficient
f = frequency (H_Z)
K = reduced frequency parameter ($\omega c/2V$)
Re = Reynolds number
V = freestream velocity (fps)
x/c = fractional chordwise distance from leading edge
α = angle of attack (degrees)
$\dot{\alpha}$ = $(\partial\alpha/\partial t)$
ΔC_p = C_p lower surface − C_p upper surface
θ = gust amplitude (± degrees)
μ = advance ratio
σ = solidity
ϕ = phase lag of gust relative to vane position (degrees)
ψ = azimuth angle measured from downstream blade position (degrees)
ω = frequency of oscillation (rads/sec)

Introduction

WITH increasing flight speed, problems associated with blade stall flutter on the retreating blades of helicopter rotors have become increasingly significant. In order to maintain equilibrium in roll the retreating blade must have a significantly greater angle of attack than the advancing blade, often considerably above the static stall angle. Typical cyclic variations of angle of attack for a real rotor in flight[1] are shown in Fig. 1.

Considerable effort both theoretically[2-8] and experimentally[9-11] is being expended in attempts to determine the magnitudes of the transient loads, the mechanisms leading to, and causes of the overshoot involved in dynamic stall. This paper discusses experimental results for the first of the above.

Although some measurements have been made on actual rotors[8] more data have been obtained from wind-tunnel tests, like those at Texas A&M University, using two-dimensional airfoils.[9,10] Other workers have used an oscillating airfoil in a steady stream, so part of the current work was to compare results for an oscillating airfoil in a fixed stream with a fixed airfoil in an oscillating stream.

Received September 4, 1973; revision received March 28, 1974. This work was sponsored by the U.S. Army Research Office-Durham under Project Themis Contract DAHCO-4-69-C-0015.
Index categories: Nonsteady Aerodynamics; Research Facilities and Instrumentation; Rotary Wing Aerodynamics.
*Assistant Professor. Member AIAA.
†Visiting Professor. Member AIAA.

Equipment and Tests

To obtain the oscillatory flow, a stream oscillation apparatus was developed[12] at TAMU. A schematic of the system as installed in the 7′ × 10′ low speed tunnel is shown in Fig. 2. Two vanes with forty per cent flaps are mounted vertically in the throat of the tunnel, the test section sides of which have been removed. Flap angle is varied sinusoidally by a variable speed electric motor and produces sinusoidal oscillations in the airstream near the

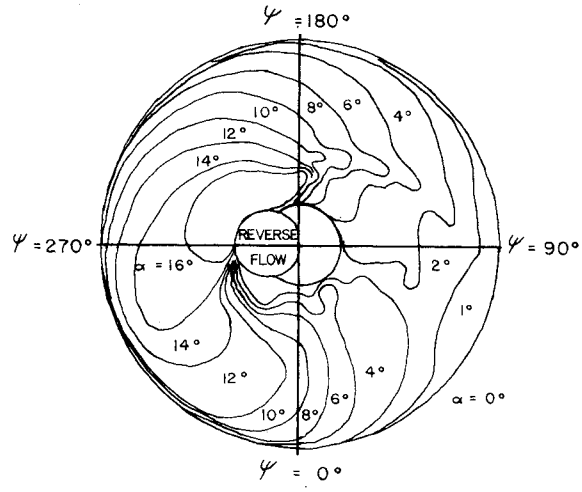

Fig. 1 Angle-of-attack distribution with nonuniform downwash. Vertol model CH-47A, front rotor, V = 140 knots, forward c.g. position, gross weight = 27,500 lb (μ = 0.33).

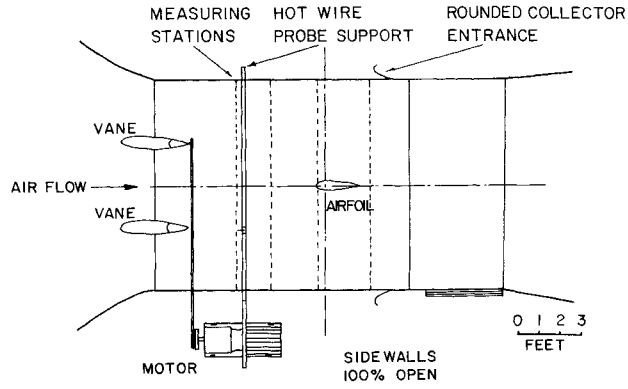

Fig. 2 Plan view of gust generator and airfoil.

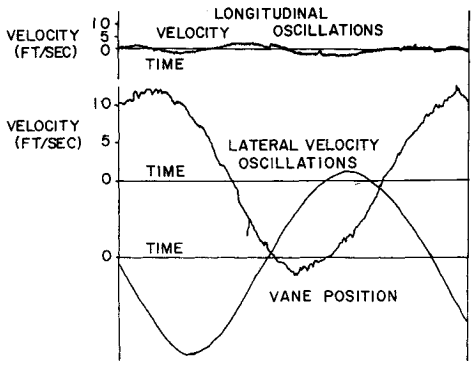

Fig. 3 Typical velocity fluctuations. Mean longitudinal velocity = 90 fp. Frequency parameter $K = 0.12\ \text{ft}^{-1}$.

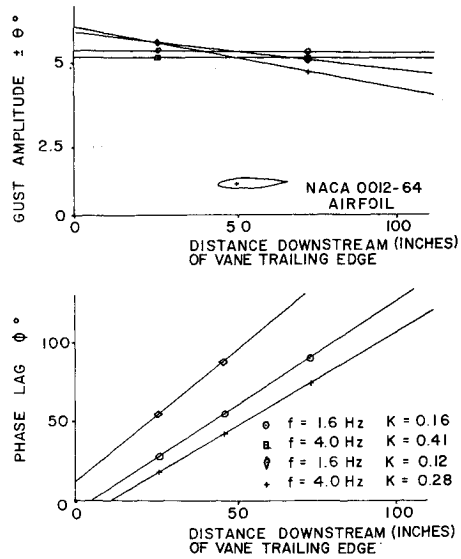

Fig. 4 Amplitude and phase variations.

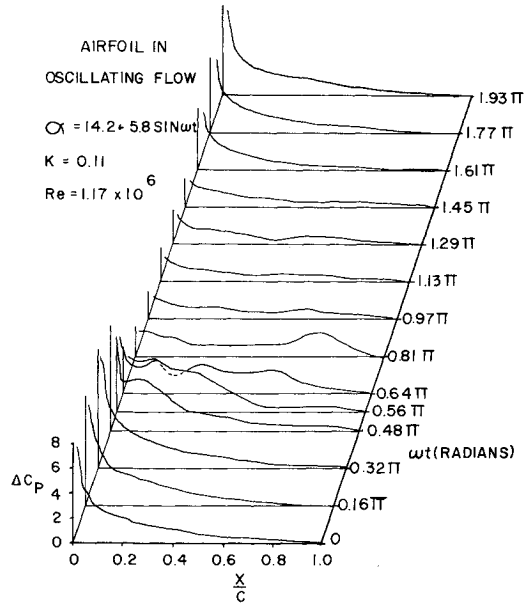

Fig. 5 Time-dependent variation of chord loading.

center of the test section (Fig. 3). Amplitude is almost constant in the test area (Fig. 4) for a given flap angle amplitude, but can be changed by altering that amplitude.

A two-foot chord two-dimensional NACA 0012-64 airfoil instrumented with twelve pressure transducers connected

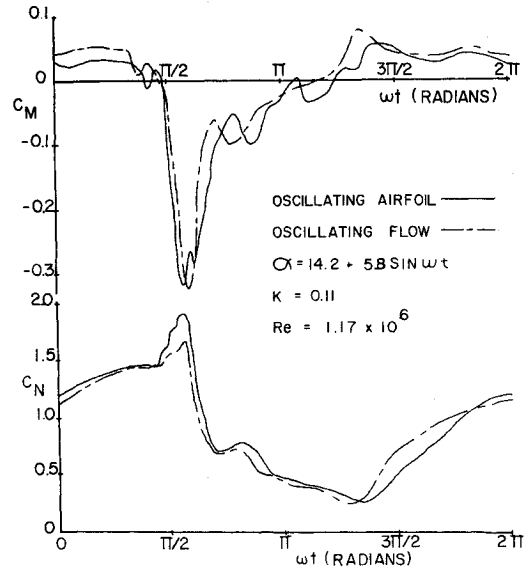

Fig. 6 Variations of pitching moment and normal force with time.

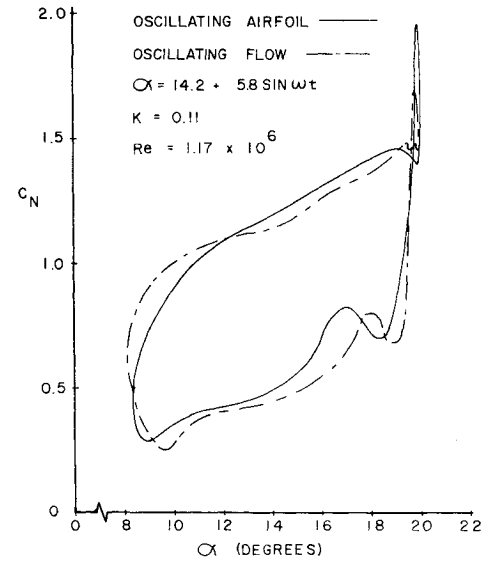

Fig. 7 C_N vs α; $K = 0.11$.

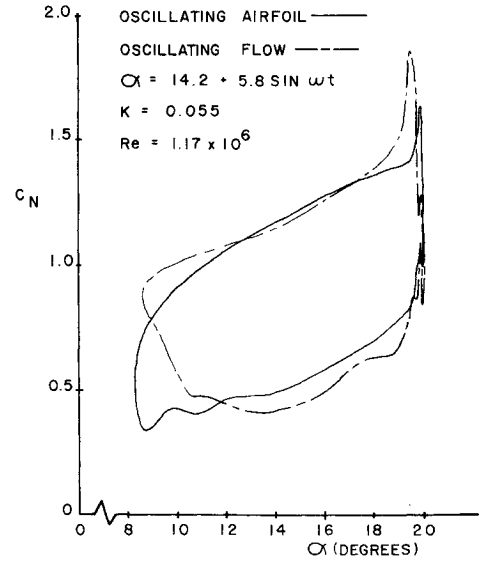

Fig. 8 C_N vs α; $K = 0.055$.

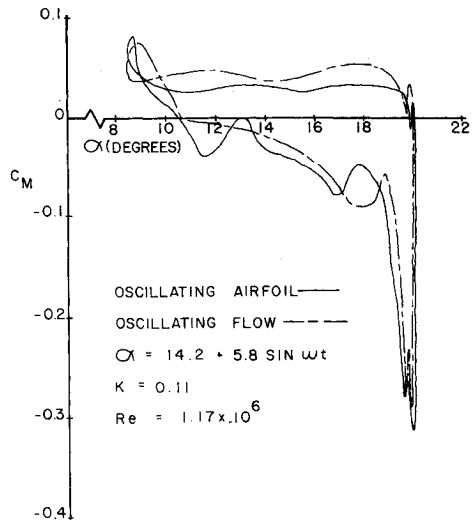

Fig. 9 C_M vs α; $K = 0.11$.

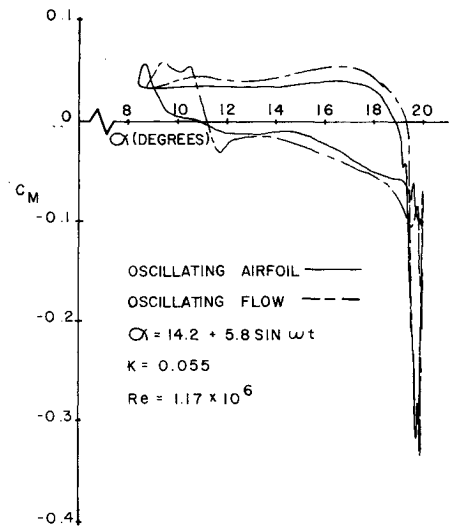

Fig. 10 C_M vs α; $K = 0.055$.

between the upper and lower surfaces was mounted in this flow and data taken for several mean angles of attack up to and beyond those necessary to produce dynamic stall. From time histories of the pressure variations at each pressure port on the wing, time histories of the chordwise load distribution (Fig. 5), normal force and pitching moment were obtained. This process of data reduction was very tedious so an operational amplifier summing system was developed into which all channels of pressure data were fed and out of which direct time histories of normal force and pitching moments were obtained. Typical traces for these electronically summed forces and moments (about the quarter chord) are shown in Fig. 6.

Having acquired data for the oscillating flow case, the airfoil itself was pivoted at its quarter-chord point and oscillated in pitch over a comparable set of test conditions. Prior to the tests, care was taken to align the transducer diaphragms normal to the direction of motion, checks revealed no measureable outputs due to inertial loads. Normal force and pitching moment curves are shown in Fig. 6.

Since the above tests were conducted in an open-sided wind tunnel, a significant amount of stream curvature occurred, particularly with the airfoil at high angles of attack (approximately 5° at $\alpha = 20°$). In steady flow, corrections to angle of attack can be applied;[13] however extending the computation of the corrections to an unsteady flow with large separated regions, due to stall, was beyond the authors' capabilities. Therefore since some corrections were required and the frequency was low it was decided, though not rigorously justified, to apply steady flow corrections to the oscillatory results. All the data presented has these corrections applied. From the data presented in Fig. 6, curves of $C_N \sim \alpha$, $C_M \sim \alpha$, and $C_N \sim C_M$ were plotted (Figs. 7–11).

Discussion

The chordwise loading distributions of Fig. 5 indicate conventional increasing loading distributions up to the point of moment stall ($\omega t \simeq (\pi/2)$, $\alpha \simeq 20°$) at which point the suction peak starts decreasing, broadening, and moving aft, as a result of the shedding of a strong leading edge vortex. At successive time intervals, this peak moves further aft but is followed by several other smaller suction peaks that also progress towards the trailing edge. This would seem to indicate that more than one vortex is shed during the stall process, a point also noted by Martin et al.[9] The exact reattachment point is difficult to identify but occurs at approximately $\omega t = 1.4\pi$, $\alpha = 8.75°$.

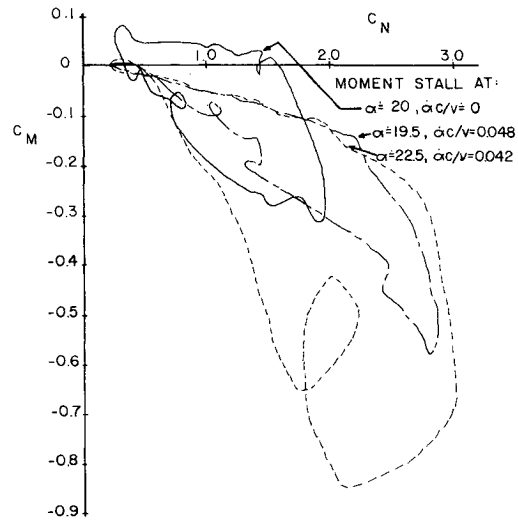

Fig. 11 Comparison of $C_M \sim C_N$ curves. —— Present tests $\alpha = 14.2 + 5.8 \sin \omega t$, $k = 0.11$, $Re = 1.17 \times 10^6$. - - - Ref. 9 $\alpha = 15 + 14 \sin \omega t$, $k = 0.1$, $Re = 10^6$. – – – Ref. 8 $C_T/\sigma = 0.132$, $\mu = 0.35$, $Re = 0.35, \times 10^6$.

The apparent shedding of more than one vortex would also explain the series of dips in the C_M time history curve (Fig. 6) after the main moment stall has occurred. Figure 6 also shows the closeness of results obtained from the two testing methods indicating that either method can be used to approximate the rotor environment at least for two-dimensional testing. Discrepancies between results for the two methods are smaller than cyclic variations observed in either method.

Curves of $C_N \sim \alpha$ (Figs. 7 and 8) exhibit the large hysteresis expected but at the higher frequency parameter ($K = 0.11$, Fig. 7) there is a loop in the curve near α max that was present in all the current tests and has been observed by other workers.[14,15] A possible explanation of this is that stall was occurring very close to the point of α max, consequently any overshoot of buildup of C_N would cause C_N to continue increasing while α started decreasing. The loop is not present on the results for the lower frequency ($K = 0.055$, Fig. 8) as stall occurs at a lower angle of attack, however, there is still a very rapid increase in C_N just before the stall followed by several rapid oscillations.

In the $C_M \sim \alpha$ curves (Figs. 9 and 10) the reverse is true, the loop is on the low-frequency results (see also Ref. 16). However, the above argument still applies if moment stall

occurs right on the point of α max as it does for the high frequency, then α starts decreasing just after C_M starts dropping, if moment stall occurs slightly before α max (low-frequency case) then C_M has reached a minimum and started increasing again before α starts decreasing. Like the results of Martin et al.,[9] Figs. 7–10 show that stall occurs at lower angles of attack for the lower frequency parameter but unlike Martin's results, the present tests show no significant variations (i.e., within the range of cyclic repeatability) with K in the values of C_N max and C_M min.

The reason the rapid oscillations apparent in Figs. 6–10 have not appeared in other workers might be due to the fact that in the current tests C_M and C_N were recorded continuously rather than obtained at a finite number of time increments.

Figure 11 shows a comparison of $C_M \sim C_N$ between present results for an oscillating airfoil and results from Refs. 8 and 9. The fact that the size of the hysteresis loop is much smaller for the present tests is almost certainly due to the much smaller amplitude of oscillation. An interesting point is that the angle of attack at which moment stall occurs is close to that obtained in Ref. 8 and 9 despite the fact that in the present tests, $\dot{\alpha}c/V$ had almost dropped to zero at the moment of stall. On the present data, the loop in the curve at the instant of stall was there in all tests of $K = 0.11$.

Conclusions

It has been adequately demonstrated that the method of oscillating an airstream rather than an airfoil produces the same results within the range of cyclic response repeatability of the aerodynamic phenomena, this leaves the way open to a lot more research in this field since it is often easier to instrument a stationary model than an oscillating one.

The dynamic stall process is accompanied by the shedding of several vortices from the leading edge resulting in very rapid sometimes oscillatory changes in C_N and C_M. Because of the rapidity of these changes, data reduced from pressure distributions at a finite number of steps could yield misleading information. Increasing the frequency parameter increases the stall delay, but in these tests did not produce a significant change in C_N max or C_M min.

Exact reasons for the stall delay are still unknown and will probably remain so until detailed boundary-layer measurements on an oscillating airfoil are made in the region of the laminar separation bubble. Since the bubble is small (1% – 2% of chord length) much larger wings than are currently being used will have to be tested in order to make accurate measurements possible.

As yet the authors know of no results indicating the effects of tunnel wall constraints (either closed or open) on the dynamic stall process. Work on this problem is currently underway at Texas A&M.

References

[1]Ham, N. D., "Helicopter Blade Flutter," *AGARD Manual of Aeroelasticity*, Vol. 3, Sept. 1967, Chap. 10.

[2]McCroskey, W. J. and Yaggy, P. F., "Laminar Boundary Layers On Helicopter Rotors in Forward Flight," *AIAA Journal*, Vol. 6 No. 10, Oct. 1968, pp. 1919–1926.

[3]McCroskey, W. J., "The Inviscid Flowfield of an Unsteady Airfoil," *AIAA Journal*, Vol. 11, No. 8, Aug. 1973, pp. 1130–1136.

[4]Ericsson, L. E. and Reding, P. J., "Analytic Prediction of Dynamic Stall Characteristics," AIAA Paper 72-682, New York, 1972.

[5]Chu, W. H., "Unsteady Boundary-Layer Flow over an Oscillating Thin Foil," *Journal of Hydronautics*, Vol. 2, No. 2, April 1968, pp. 93–101.

[6]Johnson, W. and Ham, N. D., "On the Mechanism of Dynamic Stall," *Journal of the American Helicopter Society*, Vol. 17, Oct. 1972, pp. 36–45.

[7]Patay, S., "Leading Edge Separation on an Airfoil During Dynamic Stall," MIT Rept. ASRL-TR-156-1, Oct. 1969, MIT, Cambridge, Mass.

[8]Jones, W. P., McCroskey, W. J., and Costes, J. J., "Unsteady Aerodynamics of Helicopter Rotors," AGARD 595, April 1972.

[9]McCroskey, W. J. and Fisher, R. K. Jr., "Detailed Aerodynamic Measurements on a Model Rotor in the Blade Stall Regime," *Journal of the American Helicopter Society*, Jan. 1972, pp. 20–30.

[10]Martin, J. M., Empey, R. W., McCroskey, W. J., and Cavadonna, F. X., "A Detailed Experimental Analysis of Dynamic Stall on an Unsteady Two-Dimensional Airfoil," *29th Annual National Forum of the American Helicopter Society*, Preprint 702, May 1973.

[11]Ham, N. D. and Garelich, M. S., "Dynamic Stall Considerations in Helicopter Rotors," *Journal of the American Helicopter Society*, Vol. 13, April 1968, pp. 49–55.

[12]Bicknell, J. and Parker, A. G., "A Wind Tunnel Stream Oscillation Apparatus," *Journal of Aircraft*, Vol. 9, No. 6, June 1972, pp. 446–447.

[13]Katzoff, S., Gardner, C. S., Diesendruck, L., and Eisenstadt, B. J., "Linear Theory of Boundary Effects in Open Wind Tunnels With Finite Jet Lengths," Rept. 976, 1950, NACA.

[14]Carta, F. O., "Unsteady Normal Force on an Airfoil in a Periodically Stalled inlet Flow," *Journal of Aircraft*, Vol. 6, No. 5, Sept.–Oct. 1967, pp. 416–421.

[15]Ericsson, L. E., "Comment on Unsteady Airfoil Stall," *Journal of Aircraft*, Vol. 6, No. 5, Sept.–Oct. 1967, pp. 478–480.

[16]Liiva, J. "Unsteady Aerodynamic and Stall Effects on Helicopter Rotor Blade Airfoil Sections," *Journal of Aircraft*, Vol. 8, No. 1, Jan.–Feb. 1969, pp. 46–51.